An informational approach to the Network Disease Hypothesis in resting state fMRI

Jaime Gomez-Ramirez, Yujie Li, Qiong Wu, Xiaoyu Tang, Jinglong Wu

Abstract Here we combine graph and information theory based approaches to understand network robustness in resting state-fMRI (R-fMRI). We calculate how the network robustness is affected upon the removal of nodes in the functional connectivity network in resting state for both young and elder subjects. We argue that the discovery of network based biomarkers for neurodegenerative conditions will rely on the combination of both graph theoretic and informational approaches in R-fMRI.

Key words: resting state fMRI, network degeneration hypothesis, Markov chain, relative entropy

1 Introduction

It has been suggested that fluctuations in the BOLD signal measured in humans in resting state, represent the neuronal activity baseline and shape spatially consistent patterns [1], [2]. These slow fluctuations in the BOLD signal found in resting subjects, are highly coherent within either structural or functional networks in the human brain. Therefore, exploring these fluctuations could lead to a better understanding of the brain's intrinsic or spontaneous neural activity. Functional correlation based on the synchrony of low-frequency blood flow fluctuations in resting state, have been identified in the sensorimotor [3], visual [4], language [5], auditory [6], dorsal and ventral attention [7] and the frontoparietal control system [8]. The systematic study of those patterns using correlation analysis techniques has identi-

Biomedical Engineering Laboratory, Okayama University, Japan
Autonomous Systems Laboratory, Universidad Politécnica de Madrid, Spain
e-mail: jd.gomez@upm.es

fied a number of resting state networks, which are functionally relevant networks found in subjects in the absence of either goal directed-task or external stimuli.

The visual identification of the overall connectivity patters in resting state functional magnetic resonance imaging (R-fMRI), has been assessed using either model-based and model-free approaches. In the former, statistical parametric maps of brain activation are built upon voxel-wise analysis location. This approach has been successful in the identification of motor networks, but it shows important limitations when the seed voxel cannot be easily identified. For example, in brain areas with unclear boundaries i.e., cognitive networks involved for instance, in language or memory. Independent Component Analysis (ICA), on the other hand, is a model-free approach that allows separating resting fluctuations from other signal variations, resulting on a collection of spatial maps, one for each independent component, that represent functionally relevant networks in the brain. While ICA has the advantage over model-free methods that it is unbiased, (that is, it does not need to posit a specific temporal model of correlation between ROIs), the functional relevance of the different components is, however, computed relative to their resemblance to a number of networks based on criteria that are not easily formalized.

More recently, researchers using graph-theory based methods have been able to not only visualize brain networks, but to quantify their topological properties. Large-scale anatomical connectivity analysis in the mammalian brain, shows that brain topology is neither random nor regular. Instead, small world architectures [9] -highly clustered nodes connected thorough relatively short paths- have been identified in brain networks. Small world networks are not solely structural, functional networks with a small world organization have been identified in the mammal brain [10]. In addition to this, disruptions in the small world organization can give clues about normal development and pathological conditions. For example, Supekar and colleagues [11] have shown that the deterioration of small world properties such as the lowering of the cluster coefficient, affect local network connectivity, which in turn may work as a network biomarker for Alzheimer's disease. Abnormalities in small-worldness may also have a significant positive correlation in, for example, schizophrenia [12] and epilepsy [13]. While network-based studies have been successful in delineating generic network properties, such as path length or clustering, additional work is needed in order to come to grips with the internal working of the systems underlying the network.

Robustness in brain connectivity has been typically approached in terms of the impact that the complete disruption and/or removal of a network component has in the network topology [14]. However, by focusing on the topology of the network, factors that may play a key role in the network's vulnerability to failures can be neglected. For example, it has been suggested that patients with Alzheimer's disease show an increment in brain activity in certain areas relative to healthy subjects that compensates for the disease related atrophy of other regions [15]. The network degeneration hypothesis, NDH for short, encompasses the idea that neurodegeneration can be studied as a network dysfunction process, in which changes in the network organization are informative about the progression of the disease [16], [17]. The network degeneration hypothesis -disease starts in small network assemblies,

to progressively spread to connected areas of the initial locus- has been investigated in a number of brain pathologies including Alzheimer's disease [18], epilepsy [13], schizophrenia [12] and unipolar depression [19]. To our knowledge, the first attempt to systematically test the NDH is in [16], in which Seeley and colleagues use functional and structural network mapping approaches to characterize five distinct neurodegenerative syndromes.

In this paper we explore the network degeneration hypothesis using a methodology that combines graph and information theoretic tools. In section 2 the methodology followed in the data acquisition, data preprocessing, anatomical parcellation and brain network reconstruction in two groups -24 young and 19 elder individuals- is presented. Then we systematically study network robustness -functional network invariance under perturbation- is affected upon the removal of nodes in the functional connectivity network in resting state for both young and elder subjects. We provide a ranking of nodes that quantifies the impact of their obliteration using a network efficiency measure based on [20] that quantifies how the network efficiency in transmitting information deteriorates once a node is removed from the network. This is described in the results section 3. The paper concludes with a discussion section 4 in which it is sketched a new theoretical framework to investigate network robustness and how it is affected by internal perturbations such as aging and neurological disorders.

2 Materials and Methods

2.1 Subjects

Twenty-three healthy male volunteers (ages 21-32; mean 22.7) took part in the fMRI experiment. All subjects had normal or corrected-to-normal vision. The study was approved by the ethics committee of Okayama University, and written informed consent was obtained before the study.

2.2 Data acquisition

All subjects were imaged using a 1.5 T Philips scanner vision whole-body MRI system (Okayama University Hospital, Okayama, Japan), which was equipped with a head coil. Functional MR images were acquired during rest when subjects were instructed to keep their eyes closed and not to think of anything in particular. The imaging area consisted of 32 functional gradient-echo planar imaging (EPI) axial slices (voxel size=3x3x4 mm3, TR=3000 ms, TE=50 ms, FA=90^o, 64x64 matrix) that were used to obtain T2*-weighted fMRI images in the axial plane. We obtained 176 functional volumes and excluded the first 4 scans from analysis. Before the

EPI scan, a T1-weighted 3D magnetization-prepared rapid acquisition gradient echo (MP-RAGE) sequence was acquired (TR=2300 ms, TE=2.98 ms, TI=900 ms, voxel size=1x1x1 mm3).

2.3 Data preprocessing

Data were preprocessed using Statistical Parametric Mapping software SPM8 [1] and REST v1.7 [2]. To correct for differences in slice acquisition time, all images were synchronized to the middle slice. Subsequently, images were spatially realigned to the first volume due to head motion. None of the subjects had head movements exceeding 2.5 mm on any axis or rotations greater than 2.5^{o}. After the correction, the imaging data were normalized to the Montreal Neurological Institute (MNI) EPI template supplied with SPM8 (resampled to 2x2x2 mm3 voxels) [3]. In order to avoid artificially introducing local spatial correlation, the normalized images were not smoothed. Finally, the resulting data were temporally band-pass filtered (0.01-0.08 Hz) to reduce the effects of low-frequency drifts and high-frequency physiological noises [21].

2.4 Anatomical parcellation

Before whole brain parcellation, several sources of spurious variance including the estimated head motion parameters, the global brain signal and the average time series in the cerebrospinal fluid and white matter regions were removed from the data through linear regression [**?**]. Then, the fMRI data were parcellated into 90 regions using an automated anatomical labeling template [**?**]. For each subject, the mean time series of each region was obtained by simply averaging the time series of all voxels within that region.

2.5 Brain network construction

To measure the functional connectivity among regions, we calculated the Pearson correlation coefficients between any possible pair of regional time series, and then obtained a temporal correlation matrix $(90x90)$ for each subject. We applied Fisher's r-to-z transformation to improve the normality of the correlation matrix. Then, two-tailed one-sample t-tests were performed for all the possible 4005 i.e., $\frac{90x89}{2}$ pairwise

[1] http://www.fil.ion.ucl.ac.uk/spm/

[2] http://restfmri.net/forum/index.php

[3] http://imaging.mrc-cbu.cam.ac.uk/imaging/Templates

correlations across subjects to examine whether each inter-regional correlation significantly differed from zero.

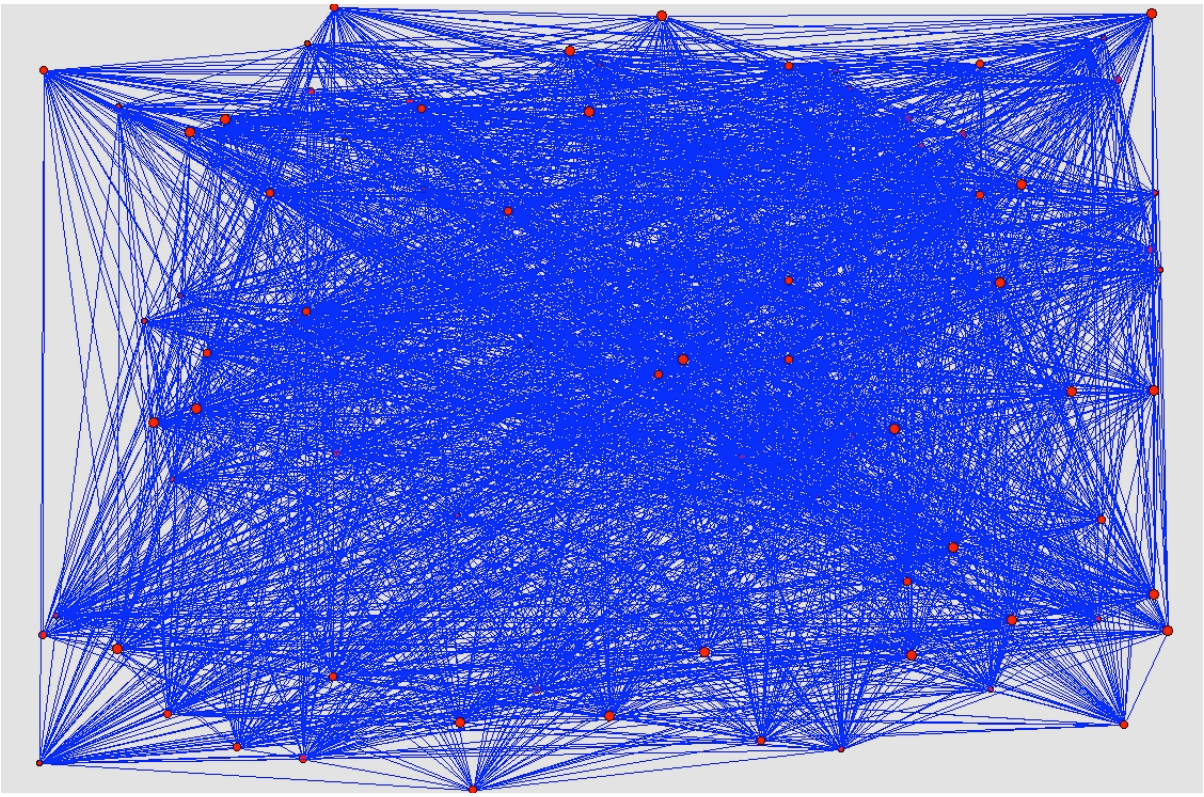

Fig. 1 Graphic representation of the functional connectivity among regions based on the temporal correlation matrix of the twenty-three healthy controls, using Pajek software [22]

A Bonferroni-corrected significance level of $P < 0.001$ was further used to threshold the correlation matrix into an adjacency matrix whose element was 1 if there was significant correlation between the two brain regions and 0 otherwise. Finally, an undirected binary graph was acquired in which nodes represent brain regions and edges represent links between regions. The study of the connectivity distribution of the resulting adjacency matrix is provided in the Appendix **??**.

2.6 Graph theoretic analysis

Until the recent advent of graph theoretic methods in R-fMRI, the focus was put on the identification of anatomically separated regions that show a high level of functional correlation during rest. The tools we use to model a system may also convey an ontological version of it, that is to say, the system under study is seen through the lens of a specific approach that necessarily shapes the observability domain. Thus, the identification of different subnetworks during rest can be seen as a by-product of the techniques used, for example identification component analysis (ICA) or clustering. Graph theory provides a theoretical framework to investigate the overall architecture of the brain. The use of graph theoretic techniques to model brain networks has shifted the emphasis from the identification of local subnetworks -default mode network, primary sensory motor network etc.- to the quantitative study of the topological and informational characteristics of large-scale brain networks. Graph theory-based approaches model the brain as a complex network in which nodes represent brain regions of interest and the edges connecting nodes represent relationship between nodes e.g., functional connectivity.

The graph-based network provides a geometric representation to visualize brain connectivity patterns and an analytic toolbox to quantitatively characterize the overall topological organization. Graph-based techniques have proliferated in the last years providing new insights into the structure function relationship in the healthy brain, and in aging and neuropathological disorders [23], [24], [25]. Prove of the utility of this approach is that notable proponents of a modularist vision of brain connectivity to understand cognition, such as Gazzaniga [26] (see [27] for an early critic of the modularist approach and anticipating a shift toward a networks) has now embraced the complex brain networks approach to understand the interplay between structure and function in brain systems [28].

2.6.1 Network robustness, efficiency and node vulnerability

A critical aspect is to understand network robustness, that is, functional network invariance under perturbation. In essence, robustness measures the capacity of the network to perform the same function before and after a perturbation. Perturbations are events, internal or external, that elicit a change in the network configuration, as for example in, to obliterate a node or a change in the connectivity between nodes. Thus, for a given network $G(N,E)$ with an adjacency matrix A, a perturbation δ (e.g., the removal of a set of nodes M from N) transforms A into a new adjacency matrix A'. Thus, the initial graph $G(N,E)$ is transformed into a new post perturbation graph $G(N-M,E-E(M))$, where $E-E(M)$ is the set of edges that do not connect any of the deleted nodes in M. Now we want to calculate the robustness of the network to the perturbations. Robustness is here studied as a loss in the efficiency. Thus, the robustness measure, $\mathscr{R}$ for a network G is defined as the relative performance retained or efficiency loss under a network insult i.e., a perturbation δ, that transforms the initial network G into G^{δ}.

$$\mathscr{R}^{\delta}(\mathscr{G}) = \frac{\Sigma(G^{\delta})}{\Sigma(G)} \tag{1}$$

Thus, from equation 1, a network G is considered to be robust if the network performance or efficiency $\Sigma(G)$ stays close to the original value after a perturbation, ideally $\mathscr{R}^{\delta} = 1$.

Now, we need to provide the formal definition of network efficiency. The efficiency of a network G ,$\Sigma(G)$, is a network centrality measure that quantifies how likely the network is robust to the deletion of nodes i.e., the network's reliability in transmitting information, once a node or a set of nodes are removed. The network efficiency can be calculated using the Latora and Marchiori measure [20]. Acordingly, the efficiency of the graph $G(N,E)$, $\Sigma(G(N,E))$, is

$$\Sigma(G) = \frac{1}{n(n-1)\sum_{i\neq j\in N}\frac{1}{d_{ij}}} \tag{2}$$

where n is the number of nodes or $|N|$ and d_{ij} is the shortest path length (the geodesic distance) between nodes i and j. Note that $0 \leq d_{ij} = d_{ji} \leq 1$. According to equation 2, a network G with an average distance between any pair of nodes $\Sigma(G) = l$ is more efficient than a network H with an average distance between any pair of nodes $\Sigma(G) = m$, if and only if $l > m$. The global network efficiency is 0.3678 for young subjects and 0.1144 for elder subjects. Thus, young subjects connecivity network is three times more efficient in terms of the shortest path distance between any two nodes.

We can, in addition to robustness and efficiency which are global measures, study the vulnerability of each node. The vulnerability of a node i, $vul(i)$ represents how the deletion of node i affects the efficiency and the robustness of the resulting network.

$$vul(i) = \frac{\Sigma(G(N,E)) - \Sigma(G(N-i,E))}{\Sigma(G(N,E))} \tag{3}$$

In Table **??** (see Excel file) is shown the vulnerability value for each of the AAL regions. Interestingly, there are some nodes that when removed, the overall network vulnerability decreased -nodes 89 to 41 for young subjects and nodes 33 to 88 in the table for Elder subjects. In young subjects, the deletion of node 89 results in an increase in the overall network efficiency of a 22.7% according to the formula 3. The network vulnerability deteriorates for the the remaining 63 nodes. The worst performance occurred when nodes 60, 31, 50, 46, 73 and 30 are deleted in which case vulnerability of the overall resulting network is increased between 20% and 10%. In elder subjects, the removal of nodes 34, 24, 8 and 62 shows a loss in efficiency between 24.9% (node 34) and 31.3% (node 62).

LI: What can we find in the litterature to explain or contextualize this results?

LI: Do you think is a good idea to remove entire networks , e.g., DMN (AAL 23, 24, 25, 26) rather than single nodes as I did ?

LI: It would be nice to have MCI and AD data too. Can you provide me that? With this anlysis we maybe could be able to classify between Young, Elder, MCI and AD based on the network vulnerability.

2.7 Information theoretic analysis on Markov chains

The undirected binary graph depicted in Figure 1 is the geometric characterisation of the adjacency matrix A, in which $a_{ij} = 1$ if AAL region i and AAL region j show a significant correlation, and $a_{ij} = 0$ otherwise. We transform the binary adjacency matrix A into a weighted adjacency matrix T, where $T_{ij} = \frac{a_{ij}}{\sum_j a_{ij}}$. The new graph has the same number of nodes each with a weight $T_{ij} \geq 0$ on the link that connects node i and node j. $T_{ij} = 0$ if nodes are not connected and symmetry $T_{ij} = T_{ji}$ is also preserved.

Now, let us consider a random walk -a particle moves from node to node- on the weighted undirected graph T. Thus, a random walk $X_n X_n \in \{1,2,\ldots n\}$ is a list of nodes visited by the particle. The probability that the particle moves from i to j is given by T_{ij}. This stochastic process defines a Markov chain because the probability that that the particle moves from state n to state $n+1$ is independent of the previous states, that is, $P(X_{n+1} = x_{n+1}|X_n = x_n) = P(X_{n+1} = x_{n+1}|X_n = x_n, X_{n-1} = x_{n-1},\ldots,X_1 = x_1) \forall x_1,\ldots,x_n \in \mathscr{X}$. The stationary distribution of the random walk on the undirected graph is $\mu = \frac{k_i}{2E}$, where k_i is the connectivity degree of node i and E is the total number of links contained in the graph. Thus, the stationary distribution is given by the N (the number of nodes) dimensional vector $\mu = \{\frac{k_1}{2E}, \frac{k_2}{2E}, \ldots, \frac{k_N}{2E}$. It ought to be noted that the stationary distribution does not depend on the number of nodes, but only on the total number of links E, and the weight of the neighbor nodes. Thus, the stationary distribution holds the local property that it is not altered by changes in the weights of non neighbors nodes, while keeping the total weight of the graph constant.

The entropy rate of a stochastic process represents the rate at which the entropy of a sequence e.g., a random walk, grows with n. Formally, for the stochastic process $\mathscr{X} = \{X_1,\ldots,X_i,\ldots,X_n\}$ the entropy rate is given by

$$H(\mathscr{X}) = \lim_{n\to\inf} \frac{1}{n} H(X_1, X_2, \ldots, X_n) \tag{4}$$

For a stationary Markov chain, the entropy rate is

$$H(\mathscr{X}) = \lim_{n\to\inf} H(X_n|\, X_{n-1},\ldots,X_1) = \lim_{n\to\inf} H(X_n|X_{n-1}) = \lim_{n\to\inf} H(X_2|X_1) \tag{5}$$

The entropy rate is computed with the stationary distribution of the Markov chain μ and the transition matrix T. Then

$$H(\mathscr{X}) = -\sum_{ij} \mu_i T_{ij} \log T_{ij} \tag{6}$$

We define a Markov process for both the young subjects and the elder ones with their transition matrix given by T^y_{ij} and T^e_{ij} respectively

$$T^y_{ij} = \frac{A^y_{ij}}{\sum_j A^y_{ij}}, T^e_{ij} = \frac{A^e_{ij}}{\sum_j A^e_{ij}} \tag{7}$$

where A^y_{ij} and A^e_{ij} are the binary adjacency matrix of the young and the elder subjects. Thus, the entropy rate is

$$\begin{aligned} H(\mathscr{X}^y) &= -\sum_{ij} \mu^y_i T^y_{ij} \log T^y_{ij} \\ H(\mathscr{X}^e) &= -\sum_{ij} \mu^e_i T^e_{ij} \log T^e_{ij} \end{aligned} \tag{8}$$

where $T^y_{ij} = \frac{A^y_{ij}}{\sum_j A^y_{ij}}$ and $T^e_{ij} = \frac{A^e_{ij}}{\sum_j A^e_{ij}}$

We calculate the entropy rate for the resulting Markov process after having delete a node or a group of nodes in both young and elder subjects. Thus, the relative entropy of the stochastic process defined by the set of states $\mathscr{X}' = \mathscr{X} - X_k$ in which the set of nodes X_k and their respective edges has been removed from the initial chain $\mathscr{X}$ is

$$H(\mathscr{X}') = -\sum_{ij, i, j \notin k} \mu_i T_{ij} \log T_{ij} \tag{9}$$

Now we compare the entropy rate after deletion of each node in both young an elder subjkects and the vulnerability after node removal as calculated in Section 2.6.1.

JAIME: TO DO

3 Results

We have analyzed the functional connectivity in resting state of both young and elder individuals. The nodes representing the ninety brain regions based on the AAL parcelation have been ranked in terms of their impact in terms of network robustness upon removal. Interestingly we find that in both elder and young groups the removal of certain nodes does not necessarily triggers a decrease in network robustness, the obliteration of certain nodes may also produces a positive impact in the network function, increasing the network robustness when the node is removed. We study network robustness based on the new network efficiency/performance measure (equation 2) to investigate the network functionality when a set of nodes are obliterated. The results show that in young subjects, that the nodes with a positive impact are ...TO DO LI/JAIME compared with elder subjects ...TO DO LI/JAIME.

In the second part we use information-theoretic measures to study the impact of the removal of nodes in the network. First, we model the network flows in terms of a stationary Markov chain which describes how a particle walks randomly from node to node, in both the young and elder functional connectivity graph. The probability transition matrix is derived from the binary adjacency matrix using the local property of connectivity degree. The entropy rate of a random walk on a graph in which a node or group of nodes has been removed is calculated.

The results show that in young subjects, after he removal of the nodes with a positive impact the entropy rate is $><$? TO DO JAIME than in the case of elder subjects.

4 Discussion

References

1. M. E. Raichle and D. A. Gusnard, "Intrinsic brain activity sets the stage for expression of motivated behavior," *The Journal of Comparative Neurology*, vol. 493, no. 1, pp. 167–176, 2005.
2. P. Fransson, "How default is the default mode of brain function?: Further evidence from intrinsic BOLD signal fluctuations," *Neuropsychologia*, vol. 44, no. 14, pp. 2836–2845, 2006.
3. S.-M. Kokkonen, J. Nikkinen, J. Remes, J. Kantola, T. Starck, M. Haapea, J. Tuominen, O. Tervonen, and V. Kiviniemi, "Preoperative localization of the sensorimotor area using independent component analysis of resting-state fMRI," *Magnetic resonance imaging*, vol. 27, pp. 733–740, July 2009. PMID: 19110394.
4. J. S. Damoiseaux, S. A. R. B. Rombouts, F. Barkhof, P. Scheltens, C. J. Stam, S. M. Smith, and C. F. Beckmann, "Consistent resting-state networks across healthy subjects," *Proceedings of the National Academy of Sciences of the United States of America*, vol. 103, pp. 13848–13853, Sept. 2006. PMID: 16945915.
5. M. Hampson, B. S. Peterson, P. Skudlarski, J. C. Gatenby, and J. C. Gore, "Detection of functional connectivity using temporal correlations in MR images," *Human brain mapping*, vol. 15, pp. 247–262, Apr. 2002. PMID: 11835612.
6. M. D. Hunter, S. B. Eickhoff, T. W. R. Miller, T. F. D. Farrow, I. D. Wilkinson, and P. W. R. Woodruff, "Neural activity in speech-sensitive auditory cortex during silence," *Proceedings of the National Academy of Sciences of the United States of America*, vol. 103, pp. 189–194, Jan. 2006. PMID: 16371474.
7. M. D. Fox, M. Corbetta, A. Z. Snyder, J. L. Vincent, and M. E. Raichle, "Spontaneous neuronal activity distinguishes human dorsal and ventral attention systems," *Proceedings of the National Academy of Sciences of the United States of America*, vol. 103, pp. 10046–10051, June 2006. PMID: 16788060.
8. J. L. Vincent, I. Kahn, A. Z. Snyder, M. E. Raichle, and R. L. Buckner, "Evidence for a frontoparietal control system revealed by intrinsic functional connectivity," *Journal of neurophysiology*, vol. 100, pp. 3328–3342, Dec. 2008. PMID: 18799601.
9. D. Watts and S. Strogatz, "Collective dynamics of 'small-world' networks," *Nature*, vol. 393, pp. 244–442, 1998.
10. D. S. Bassett and E. Bullmore, "Small-world brain networks," *The Neuroscientist*, vol. 12, pp. 512–523, Dec. 2006.
11. K. Supekar, V. Menon, D. Rubin, M. Musen, and M. D. Greicius, "Network analysis of intrinsic functional brain connectivity in alzheimer's disease," *PLoS Computational Biology*, vol. 4, June 2008. PMID: 18584043 PMCID: PMC2435273.

12. Y. Liu, M. Liang, Y. Zhou, Y. He, Y. Hao, M. Song, C. Yu, H. Liu, Z. Liu, and T. Jiang, "Disrupted small-world networks in schizophrenia," *Brain: a journal of neurology*, vol. 131, pp. 945–961, Apr. 2008. PMID: 18299296.
13. W. Liao, Z. Zhang, Z. Pan, D. Mantini, J. Ding, X. Duan, C. Luo, G. Lu, and H. Chen, "Altered functional connectivity and small-world in mesial temporal lobe epilepsy," *PLoS ONE*, vol. 5, p. e8525, Jan. 2010.
14. M. Kaiser, R. Martin, P. Andras, and M. P. Young, "Simulation of robustness against lesions of cortical networks," *European Journal of Neuroscience*, vol. 25, no. 10, pp. 3185–3192, 2007.
15. E. J. Sanz-Arigita, M. M. Schoonheim, J. S. Damoiseaux, S. A. R. B. Rombouts, E. Maris, F. Barkhof, P. Scheltens, and C. J. Stam, "Loss of 'small-world' networks in alzheimer's disease: graph analysis of FMRI resting-state functional connectivity," *PloS One*, vol. 5, no. 11, p. e13788, 2010. PMID: 21072180.
16. W. W. Seeley, R. K. Crawford, J. Zhou, B. L. Miller, and M. D. Greicius, "Neurodegenerative diseases target large-scale human brain networks," *Neuron*, vol. 62, pp. 42–52, Apr. 2009. PMID: 19376066.
17. M. Mesulam, "Defining neurocognitive networks in the BOLD new world of computed connectivity," *Neuron*, vol. 62, pp. 1–3, Apr. 2009. PMID: 19376059.
18. R. L. Buckner, J. Sepulcre, T. Talukdar, F. M. Krienen, H. Liu, T. Hedden, J. R. Andrews-Hanna, R. A. Sperling, and K. A. Johnson, "Cortical hubs revealed by intrinsic functional connectivity: mapping, assessment of stability, and relation to alzheimer's disease," *The Journal of neuroscience: the official journal of the Society for Neuroscience*, vol. 29, pp. 1860–1873, Feb. 2009. PMID: 19211893.
19. A. Lord, D. Horn, M. Breakspear, and M. Walter, "Changes in community structure of resting state functional connectivity in unipolar depression," *PLoS ONE*, vol. 7, p. e41282, Aug. 2012.
20. V. Latora and M. Marchiori, "Efficient behavior of small-world networks," *Physical Review Letters*, vol. 87, p. 198701, Oct. 2001.
21. Q. Jiao, G. Lu, Z. Zhang, Y. Zhong, Z. Wang, Y. Guo, K. Li, M. Ding, and Y. Liu, "Granger causal influence predicts BOLD activity levels in the default mode network," *Human Brain Mapping*, vol. 32, no. 1, pp. 154–161, 2011.
22. V. Batagelj and A. Mrvar, "Pajek - analysis and visualization of large networks," in *Graph Drawing Software* (M. Jünger and P. Mutzel, eds.), Mathematics and Visualization, pp. 77–103, Springer Berlin Heidelberg, Jan. 2004.
23. D. A. Fair, A. L. Cohen, J. D. Power, N. U. F. Dosenbach, J. A. Church, F. M. Miezin, B. L. Schlaggar, and S. E. Petersen, "Functional brain networks develop from a "local to distributed" organization," *PLoS computational biology*, vol. 5, p. e1000381, May 2009. PMID: 19412534.
24. J. Wang, X. Zuo, and Y. He, "Graph-based network analysis of resting-state functional MRI," *Frontiers in systems neuroscience*, vol. 4, p. 16, 2010. PMID: 20589099.
25. Y. He and A. Evans, "Graph theoretical modeling of brain connectivity," *Current opinion in neurology*, vol. 23, pp. 341–350, Aug. 2010. PMID: 20581686.
26. M. S. Gazzaniga, ed., *The New Cognitive Neurosciences: Second Edition*. The MIT Press, 2 ed., Nov. 1999.
27. J. Fuster, "The module: crisis of a paradigm book review, "the new cognitive neurosciences" 2nd edition, m.s. gazzaniga, editor-in-chief, mit press," *Neuron*, no. 26, pp. 51–53, 2000.
28. D. S. Bassett and M. S. Gazzaniga, "Understanding complexity in the human brain," *Trends in cognitive sciences*, vol. 15, pp. 200–209, May 2011. PMID: 21497128.